

Simulating Lost Circulation Treatment at Geothermal Conditions and Comparing the Efficacy of Different Materials Utilized

William Kibikas^{1,*}, Matthew Ingraham¹, Stephen J. Bauer¹, Seiji Nakagawa², Chun Chang², Patrick Dobson², Timothy Kneafsey², Abraham Samuel³

¹Sandia National Laboratories, Albuquerque, NM 87185

²Lawrence Berkeley National Laboratory, Berkeley, CA 94720

³Geo Energize, LLC, La Quinta, CA 92253

* wmkibik@sandia.gov

Keywords: Lost circulation, flow rate, high temperature, geothermal, drilling, non-productive time,

ABSTRACT

Lost circulation, or the loss of drilling fluids while drilling, and its remedial treatment represent a significant technical and financial challenge to efficient geothermal energy production. While management of lost circulation has been conducted for more than a century, preventing fluid losses in geothermal systems presents unique technical challenges due to the rock types, flow pathways, and high pressure/temperature conditions. The different materials used to treat lost circulation are expected to vary in behavior at elevated at such extreme conditions. To understand this, a high pressure/temperature flow loop system was constructed to simulate flow conditions in a geothermal reservoir. A vessel containing a gravel pack simulating a highly fractured reservoir rock was placed in the system, and water was flowed through the pack while heated to ~190–225 °C. At these temperatures, nine tests were conducted by injecting different types of commonly used lost circulation materials mixed with xanthan gum and water into the gravel pack for a period of three days. For comparison, mixtures consisting of multiple materials were also tested to examine the impact of wider grain size distribution on clogging efficiency. Flow rate and fluid pressure were monitored throughout the tests to study how the different materials modified flow over time. After the tests, each gravel pack was dried and filled with low viscosity epoxy, then the epoxied sample was cut into sections. These sections were examined microscopically to evaluate the amount and distribution of the lost circulation materials that remained within the gravel pack clogging the pores. The experiments show how different types of lost circulation treatment materials modify flow while drilling in a high pressure/temperature geothermal system.

1. INTRODUCTION

One critical challenge for efficient and economical development of geothermal energy is the loss of fluids that occurs during drilling, referred to as lost circulation (LC) (e.g., Price et al., 2023). The occurrence of LC during geothermal drilling is a major source of non-productive time that represents on average 10–20% of the total drilling costs (Blankenship et al., 2005; Cole et al., 2017). Untreated LC during drilling can result in several complications, such as drilling mud loss, unbalanced borehole pressures, blind drilling, and wellbore collapse. In geothermal drilling LC is a much more complicated issue than in oil and gas projects, as formations are often geologically complex and require drilling toward zones of high permeability that would most likely result in LC.

LC is typically treated with the use of “lost circulation materials” (LCM) that are mixed into the drilling fluid either before encountering losses (e.g., preventative treatment) or after losses have occurred (e.g., corrective treatment). These materials are highly variable in their properties and have many classifications that have been developed to characterize them. In geothermal drilling, various materials have been utilized to treat LC, including but not limited to calcium carbonate, graphite, micronized rubber, diatomaceous earth, walnut shells, sawdust, micronized cellulose, rice husks, polymers, and various commercial blends. However, the LC treatment is often ineffective at mitigating moderate to severe fluid loss zones. In geothermal wells, the geologic complexity creates unique loss situations such that previously successful approaches in oil and gas drilling in sedimentary rocks may not work. Also, the higher temperatures can produce more rapid breakdown of many LCMs. A typical approach during geothermal drilling is to use the least costly LCM first, then use progressively more expensive materials until losses stop (Winn et al., 2023). However, Lowry et al. (2022) showed that the primary cost incurred during LC events came not through the materials used for treatment but the non-productive time spent on attempting to treat the loss zone. Given this, during geothermal drilling the important factor for reducing LC cost is to use the most effective and efficient LCM as soon as possible.

One of the limitations of LCM usage is that how and why clogging occurs is not well understood. In laboratory experiments, different LCMs in permeable zones can pass through without clogging, pile up and clog the entrance to the fluid loss zone, bridge the flow zone but still allow moderate fluid loss, or clog erratically as the fluid pressure oscillates with repeated clogging and unclogging by the LCM. Various rules have been developed to characterize the selection of an LCM for treatment, including the Abrams’ rule (i.e., median particle size of LCM equal to or greater than 1/3 of the median pore size), the Vickers Method (i.e., D90 = largest pore throat, D75 < 2/3 of largest pore throat, D50 ~ 1/3 of the mean pore throat, D25 ~ 1/7 of the mean pore throat, D10 > smallest pore throat), the Haliburton Method

(i.e., D50 of particles equal to 1/2 the estimated fracture width), and the Alsaba Method (i.e., particle size distribution of $D_{50} \geq 3/10$ of the fracture width and $D_{90} \geq 6/5$) (Abrams, 1977; Vickers et al., 2006; Whitfill, 2008; Alsaba et al., 2017).

These selection criterion for LCM however only rely on the size distribution of the particles. They do not address other characteristics such as LCM compressibility or swellability, or the unknown size of the fracture(s) causing the loss. With regard to LC during geothermal drilling, the high downhole temperatures are likely to increase the degradation and breakdown of any organic LCMs. Kibikas et al. (2023) showed that many common LCM employed in geothermal wells experience 10-50% mass loss above 100 °C, after heating for only 1 day. The reliability of an LCM for treating LC during drilling needs to account for their degradability at geothermal conditions.

This work details research on the clogging effectiveness of several common LCM at high temperatures. A high-temperature flow loop system was constructed for injecting particulates into a homogenous gravel pack at temperatures of 190-225 °C. Various LCM were injected into the gravel pack for a period of 3 days to test their clogging efficiency. Once completed the gravel samples were filled with low viscosity epoxy to preserve the trapped LCM and then cut into sections to observe the breakdown and clogging of the LCM. The effectiveness of different LCM at clogging was then compared to determine best approaches for selecting LCM for use in high temperature drilling.

2. MATERIALS AND METHODS

2.1 Selected LCM

The LCMs tested in this study were provided by Sinclair Well Products. In this work six different LCMs are tested (as well as a mixture of several types), with each shown in Figure 1. For simplicity, we adopt a classification based on appearance of the different LCM: granular, flaky, or fibrous. Various properties of the different materials are listed in Table 1.

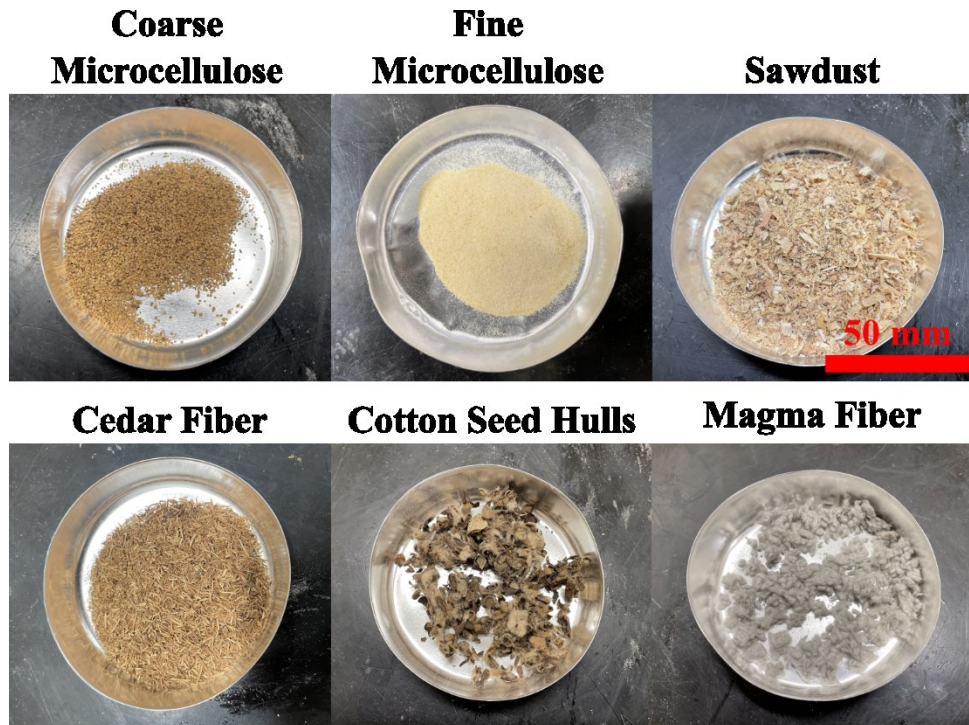


Figure 1: Image of each material utilized in LC treatment tested in this study.

LCM	Coarse Microcellulose	Fine Microcellulose	Sawdust	Cedar Fiber	Cotton Seed Hulls	Magma Fiber
Classification	Granular	Granular	Flaky/Fibrous	Fibrous	Fibrous	Fibrous

Specific Gravity (-)	1.30	1.30	0.91	0.24	0.60	2.60
Diameter (mm)	0.40-0.90	0.05-0.10	0.05-5.00	0.05-5.00	0.40-10.00	0.50-4.00
Swelling (%)	1-5	1-5	10-20	1-5	10-20	0
Description	Ground Walnut/Almond Shells	Ground Walnut/Almond Shells	Wood Dust	Ground Cedar Bark	Cotton Seed Hulls	Spun Rock Wool

Table 1: Properties and description of different LCM tested in this study.

2.2 High Temperature Flow Loop System

To test the clogging ability of the LCM mixtures, a high temperature flow loop system was developed. A schematic of this system is shown in Figure 2.

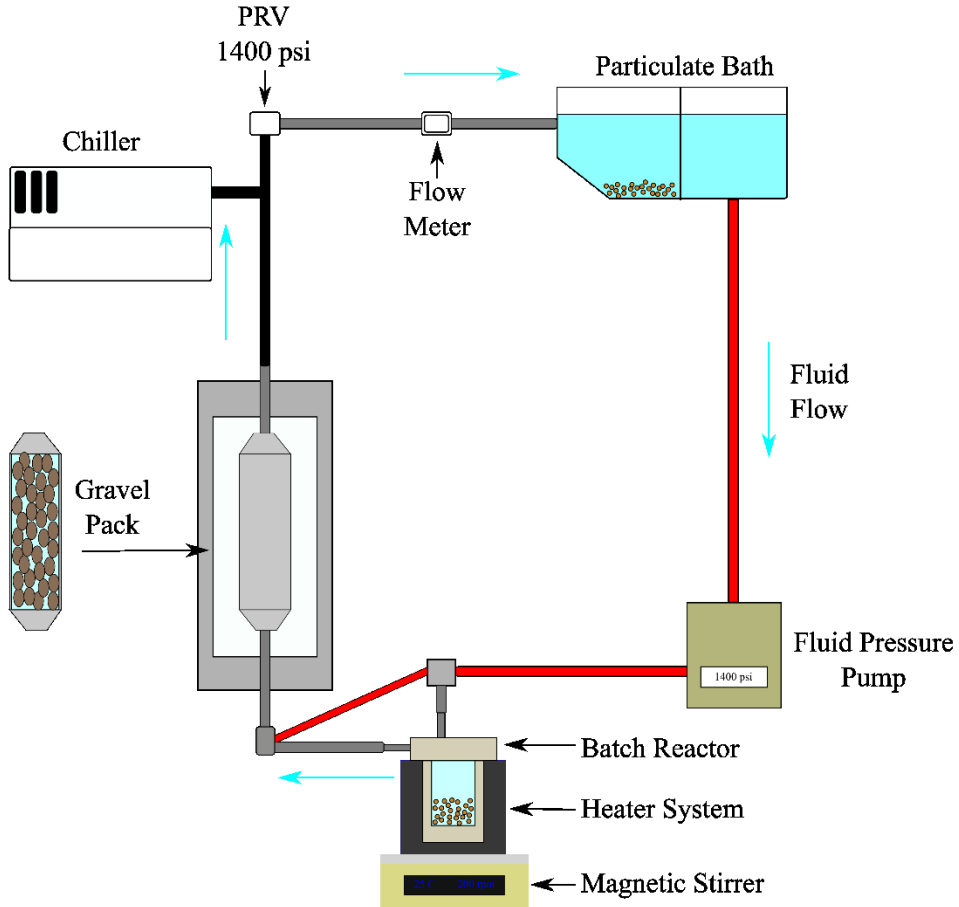


Figure 2: Schematic of flow loop system constructed. Blue arrows indicate the direction of fluid flow during testing.

The purpose of the system is to cycle water through a permeable analog system continuously while injecting different LCMs to test their different efficiency at clogging the system. The permeable system here is a gravel pack shown in Figures 2 and 3e. A stainless steel pressure vessel was constructed with a sealed internal volume of 1647 cm³. Two steel end caps act as seals at both ends, with each cap possessing a ~2.5 mm hole to allow both water and LCM to enter the gravel pack during testing. To construct the gravel pack, a silicate-rich subrounded gravel with an average grain diameter 9.5 mm was procured from Buildology in Albuquerque, NM. XRD analysis of the

gravel demonstrated a composition of 55% quartz, 28.5% albite, and 16.5% calcite. The gravel was sifted so that all the tested gravel pack possessed uniform grain diameters between 6.3-9.5 mm.

For testing, a Teflon sleeve was first placed around the rim of the gravel pack to allow for post post-test analysis, then the sifted gravel was added to the pressure vessel and packed down. Subsequently, the pressure vessel was sealed with end caps at both ends with high temperature O-rings and Teflon backup rings. Finally, the gravel pack sample was placed inside a loading frame with a heater capable of generating temperatures up to 220 °C (Figure 3b). At the top and bottom of the gravel pack, nipple seals with high temperature O-rings were connected and sealed at each end cap to allow for water flow through the system.

The main testing system has several components. The fluid pressure is provided by a Hydrorex hydrostatic pressure system (Model 10-603REX) that is able to continuously push fluid through the system. During testing, a basin of water is filled from which the Hydrorex pulls water from (Figure 3d). The system is designed so that the water flow from the Hydrorex can be diverted into either an attached batch reactor or directly into the gravel pack system. The batch reactor (Figure 3a) is a heated 4838 Parr vessel, sealed with a Teflon O-ring. During testing each LCM mixture is placed inside the batch reactor, so that heated LCM mixtures that are also thermally degraded under a designed temperature can be injected into the gravel pack. The batch reactor was seated atop an Ohaus Guardian 5000 stirring hot plate so the mixture in the reactor could be actively stirred to keep the LCM in suspension during testing. To measure the inlet pressure of the gravel pack, a pressure transducer was installed at the upstream of the gravel pack to record fluid pressure.

Once fluid and LCM flowed through the gravel pack, their temperature was reduced by a heat exchanger (ATS-Chill600V) to below the boiling point of water at atmospheric conditions. The chilled mixture then reached the downstream pressure relief valve (PRV) set at 9.65 MPa. This valve was designed so that the mixture was allowed to exit to the catchment system only when the pressure in the upstream of the PRV exceeded the set pressure, thus creating a differential pressure across the sample. In the downstream of the PRV, the mixture passed through a flow meter (Picomag DMA-15) that was used to read the flow rate in the system before the mixture entering the catchment system. Any particulates that entered the catchment system would remain trapped in one end, while the water would continue flowing through and be pulled back into the loop through the Hydrorex system.

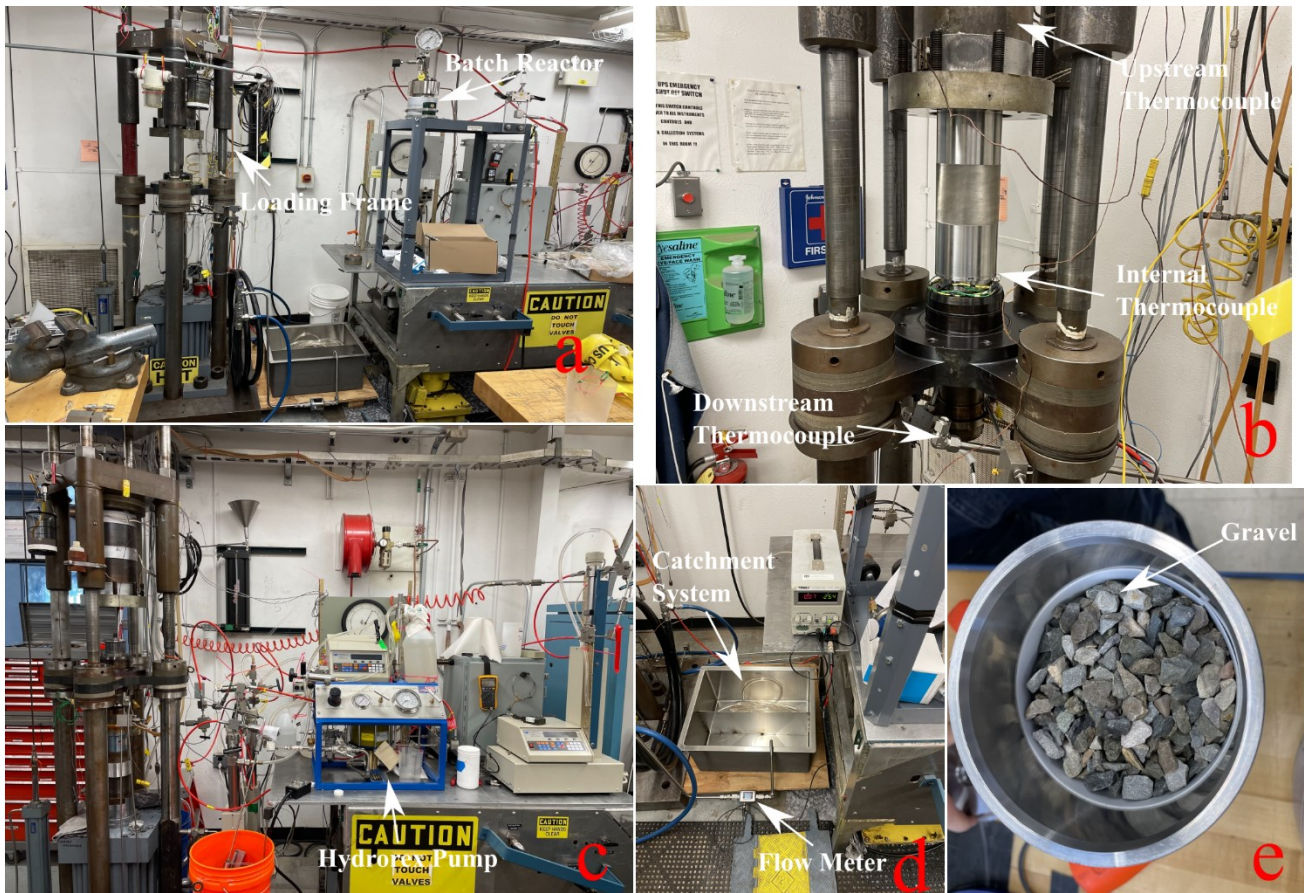


Figure 3: Photos of flow loop system equipment showing: a) the empty testing frame and batch reactor; b) gravel pack cylinder in testing frame; c) Hydrorex pressure system for maintaining constant flow through; d) flow meter and catchment tank for removing LCM that pass through gravel pack; e) untested gravel pack showing gravel and Teflon covering inside.

2.3 Flow Loop Test Procedure

The same procedure was used for each test, though in a few cases modifications had to be made due to technical difficulties. To start, the sealed gravel pack was placed in the testing frame with connections at both the top and bottom to allow water flow through. Once settled, the frame was lowered so that the outer vessel completely covered the sample. Once the frame and gravel pack were in place, the LCM mixtures were added to the batch reactor. Each LCM mixture was approximately 500 mL, with an LCM:water mass ratio of 1:4 for each mixture, that which was stirred at 200 rpm overnight. To increase the viscosity and keep the LCM in suspension during testing, 1.5 g of xanthan gum was added as a viscosifying agent to the mixture. Once prepared, the mixture and a magnetic stir bar were placed in the batch reactor and sealed, then set up in the loop system connected to the loading frame. Water was added to the catchment basin so the system could begin pumping water through.

Once ready, the Hydrorex began pumping water through the system, though not through the batch reactor, to fill it with water and test for leaks before heating. Once pressure built to 9.65 MPa upstream during the pressure cycles and no leaks were detected, flow was shut off. With the system ready, a heating blanket and shield were placed around the loading frame, then the temperature was increased. Overnight the temperature was increased and allowed to sit at 190-225 °C (varies slightly between tests). The following morning the system was opened to allow water to flow through the batch reactor into the gravel pack. Once opened, the Hydrorex was turned on and water began to flow through the system. Ideally the LCM were then pushed into the gravel pack for clogging. The flow loop was allowed to run for ~8 hours before being shut off. This was done for each day for 3 days in a row. On the 3rd day of testing, once flow was stopped, the heater for the frame was turned off and allowed to cool to room temperature overnight. The next day the setup was deconstructed, and the gravel pack sample was removed from the loading frame.

After testing, the gravel pack was opened and dried at 60 °C to remove any remaining water. Once dried, a two-component epoxy (EpoxAcast 692 Deep Pour) was mixed and poured into the gravel pack to “lock” the sample in place. After 3 days, the bottom end cap was removed and a hydraulic press was used to push out the preserved sample from steel vessel. The samples were each photographed then cut parallel and perpendicular to the long axis of the cylinder with a circular saw so the captured LCM could be observed inside each gravel pack sample.

3. EXPERIMENT RESULTS AND ANALYSIS

3.1 Flow Loop Test Results

LCM Tested	Days Tested	Max Temperature (°C)	Max Fluid Pressure (MPa)	LCM Trapped in Gravel
Water	1	185.0	9.9	No
Sawdust	3	188.9	10.1	No
Fine + Coarse Microcellulose	2	193.3	21.8	Yes
Cotton Seed Hulls	1	193.0	11.3	Yes
Cedar Fiber	3	201.1	10.6	No
Coarse Microcellulose and Cedar Fiber 1	3	217.3	10.5	No
Sawdust and Cotton Seed Hulls	3	212.2	11.2	Yes
Coarse Microcellulose and Cedar Fiber 2	3	215.7	12.2	Yes
Magma Fiber	3	224.2	10.9	Yes

Table 2: LCM tested and the parameters measured during each test.

The nine flow loop tests conducted in this work are listed in Table 2, including the materials tested, the maximum temperature experienced in the gravel pack and the maximum upstream fluid pressure during flow. Tests were conducted using both individual LCM as well as combinations of LCM, for comparison with previous experiments by Nakagawa et al. (2023). An example of the test results is shown in Figure 4, where the temperature, upstream fluid pressure, and flow rate for the cedar fiber test are shown for the entire duration of the tests.

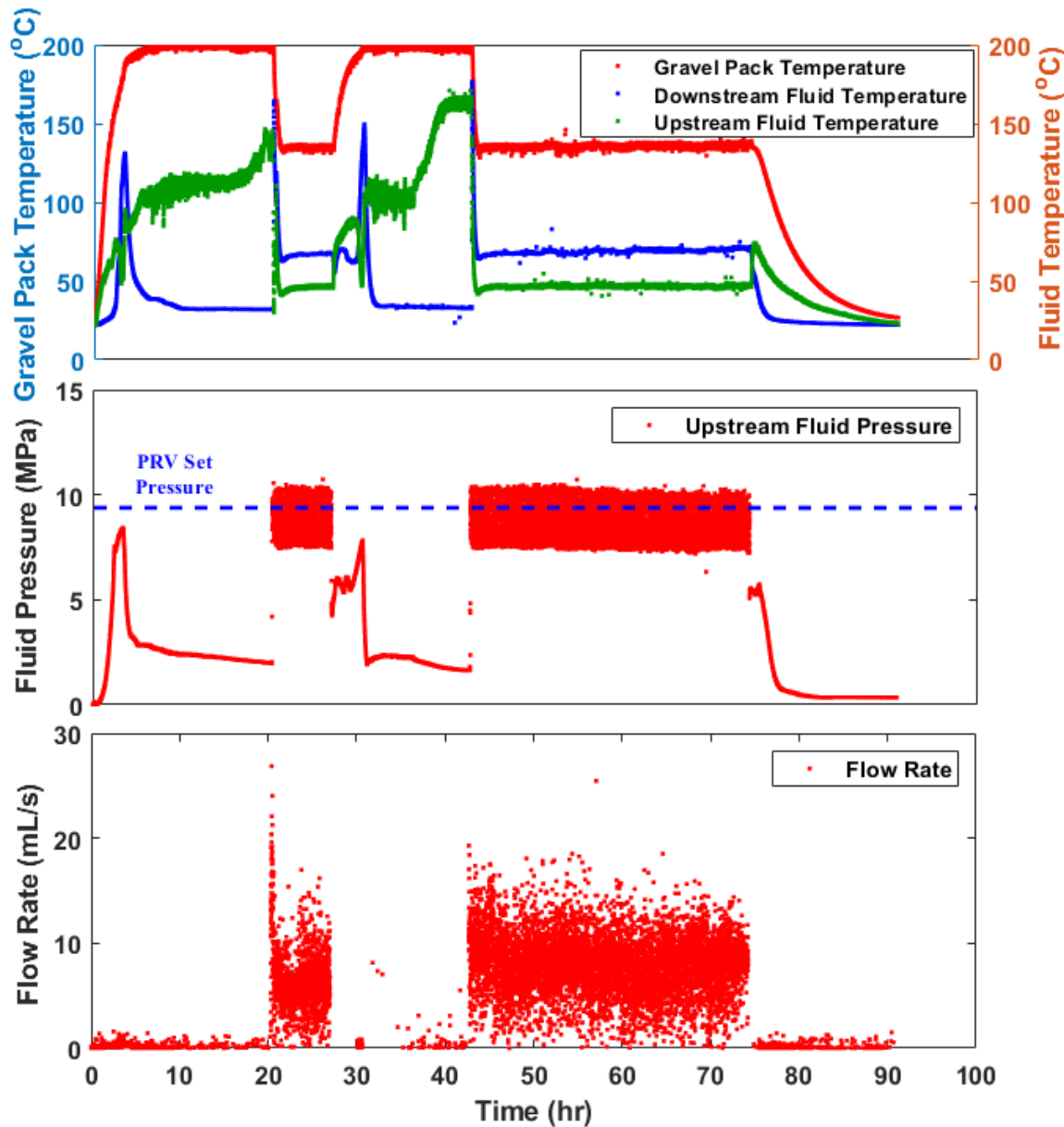


Figure 4: Example of flow loop test data for the cedar fiber test showing the temperatures, fluid pressure, and flow rate during the test. Dashed line indicates the set PRV pressure that controls the minimum pressure the system must build to in order for water to flow continue flowing through the system. Note that once PRV activates and the pressure-regulated flow starts, rapid pressure oscillation occurs in the upstream pressure. Corresponding to the changes in the induced differential pressure, flow rate in the downstream also fluctuates.

As can be seen in Figure 4, once the water flow began the gravel pack temperatures dropped from their high of 185-225 °C (Table 2) within 1-2 hours and stabilized at a lower temperature around ~130-180 °C. Once flow was halted at the end of the day, the gravel pack temperatures returned to its pre-flow level. The upstream fluid pressure in Figure 4 reflects how the system pumps water through the gravel pack, increasing the pressure until it exceeds the downstream PRV, set at 9.65 MPa, then fluid pressure drops until the PRV closes and the cycle begins again. If no clogging occurs in the gravel pack or system, as one would expect for the initial test with only water flow through, the maximum upstream fluid pressure should be only slightly greater than 9.65 MPa (Table 2). If the LCM become trapped in the gravel system and increase the pressure required to flow through the PRV, we would expect to see: 1) a maximum upstream fluid pressure more than 0.5 MPa of the set PRV and b) a flow rate lower than the average values measured for water with no clogging.

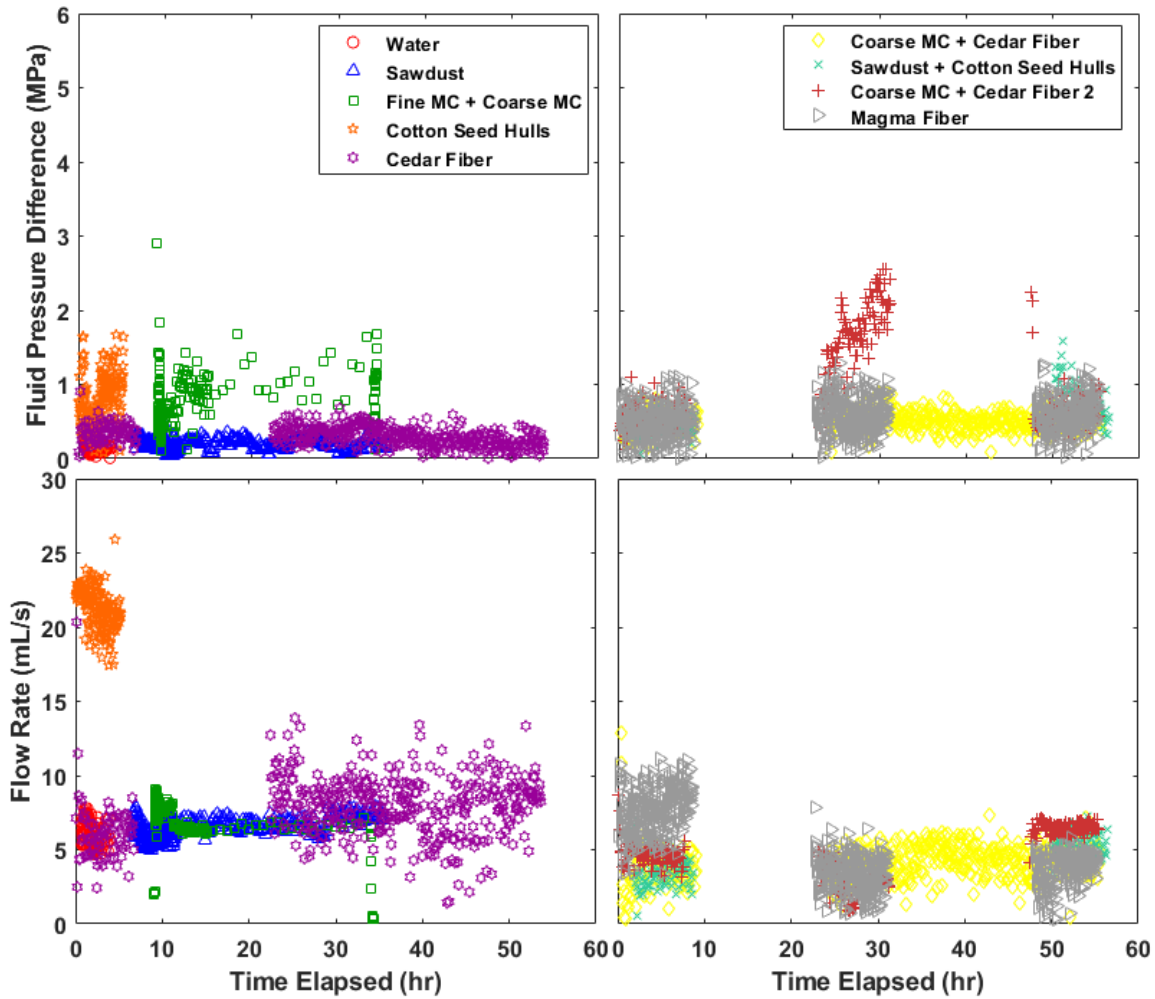


Figure 5: The differential pressure and flow rate measured during each test. Differential pressure is the difference between the downstream PRV (set to 9.65 MPa) and the pressure upstream of the gravel pack. All measurements are mean values measured every 3 minutes during the testing phase.

Since we are primarily concerned with the difference between the downstream PRV pressure and the upstream fluid pressure, we report here the fluid pressure difference (when above 9.65 MPa) to show how each LCM creates additional flow resistance through the gravel pack samples. In Figure 5, we report the fluid pressure difference and the flow rate data for each test. To eliminate outliers, the data reported here is the average of every 3 minutes of measurements.

Several observations can be made from Figure 5. The fluid pressure difference is low for the water-only test as would be expected. The sawdust and cedar fiber tests also did not experience significant pressure buildup, indicating clogging by the LCM was limited. In contrast, larger buildups of pore pressure were observed for the fine + coarse microcellulose, cotton seed hulls, sawdust + cotton seed hulls, coarse microcellulose and cedar fiber 2, and magma fiber tests, with the largest observed pressure buildup occurring in the fine + coarse microcellulose followed by the coarse microcellulose + cedar fiber 2 test. A second mixture of coarse microcellulose + cedar fiber was tested because there was a suspected hydraulic issue in flow loop, and the improved clogging observed (as evidenced by the presence of LCM in the gravel pack after the experiment) which suggests that the second test results are more valid.

The baseline flow rate obtained from the water test was around ~6 mL/s. Both the sawdust test and cedar fiber test show similar values. By contrast, the fine microcellulose + coarse microcellulose test showed a decreasing flow rate as testing continued. The flow rates measured during the cotton seed hulls test were 5-6 times the water test measurements), and the data is suspected to be in error and thus we choose to disregard it here. The cause of this anomalous behavior is unknown. The mixtures tested showed marked reductions in flow rate as testing continued, most of them decreasing from ~5 mL/s on the first day to 2.5 to 4 mL/s on the 2nd and 3rd days of flow through. The magma fiber test showed the largest drop in flow rate as pumping continued.

3.2 Post-Test Sample Analysis

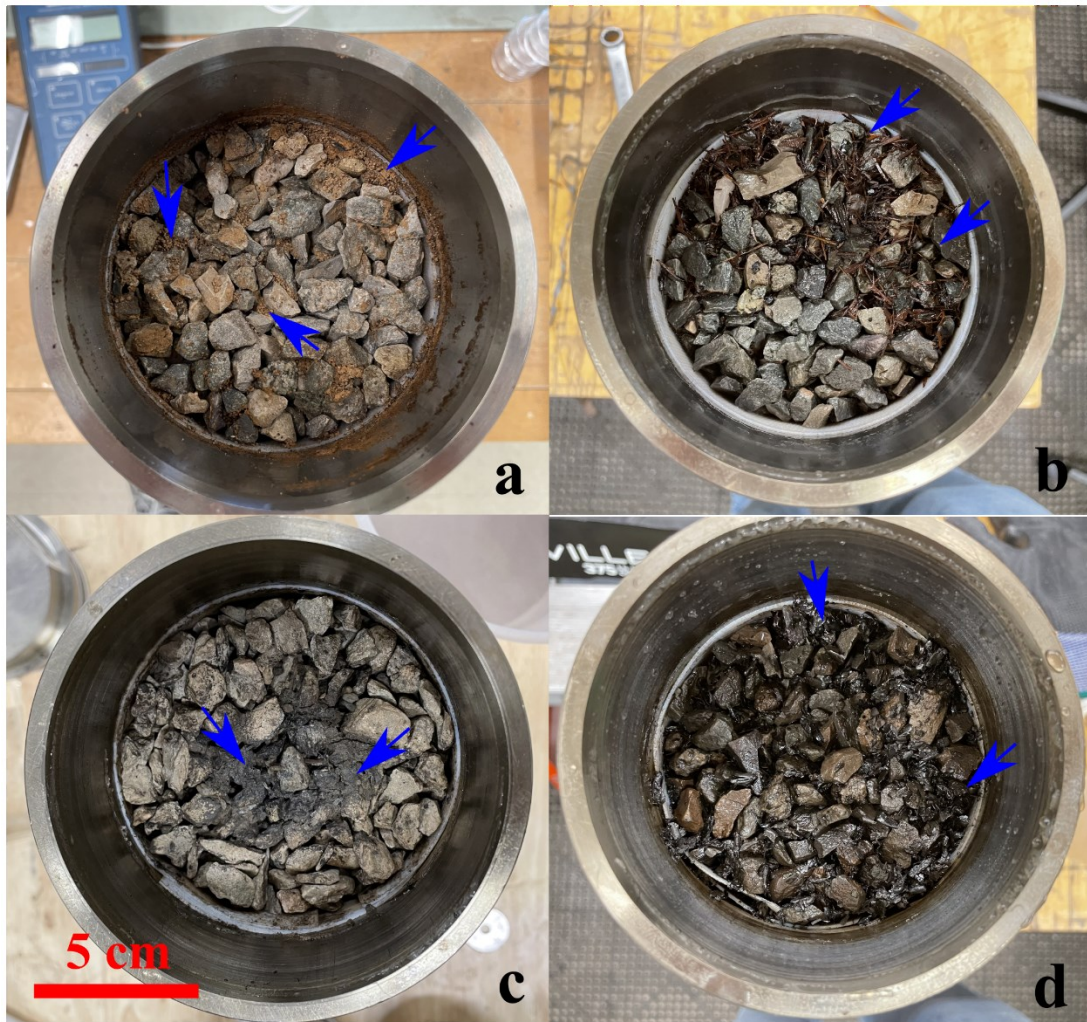


Figure 6: Examples of LCM trapped on upstream end of gravel pack for: a) fine + coarse microcellulose; b) coarse microcellulose + cedar fiber; c) magma fiber; d) sawdust + cotton seed hulls. Arrows indicate material trapped in the matrix.

When the flow-through tests were concluded, the gravel packs were removed from the system and residual water was drained. The first observation of the LCM clogging came when the top end cap of the vessels was removed to see if any LCM was trapped in the system (Table 2). No LCM was observed in the opened sawdust and cedar fiber test samples. A small amount of cotton seed hulls was observed in the tested sample, but significant amounts were observed at the top of the fine + coarse microcellulose, sawdust + cotton seed hulls, coarse microcellulose and cedar fiber 2, and magma fiber tested gravel packs (Figure 6). All the LCM observed show some degree of thermal degradation from the high temperatures. In particular, the magma fiber (Figure 6c) appears less as a fibrous material and more as a loose mesh or powdered material surrounding the entrance port for the gravel pack.

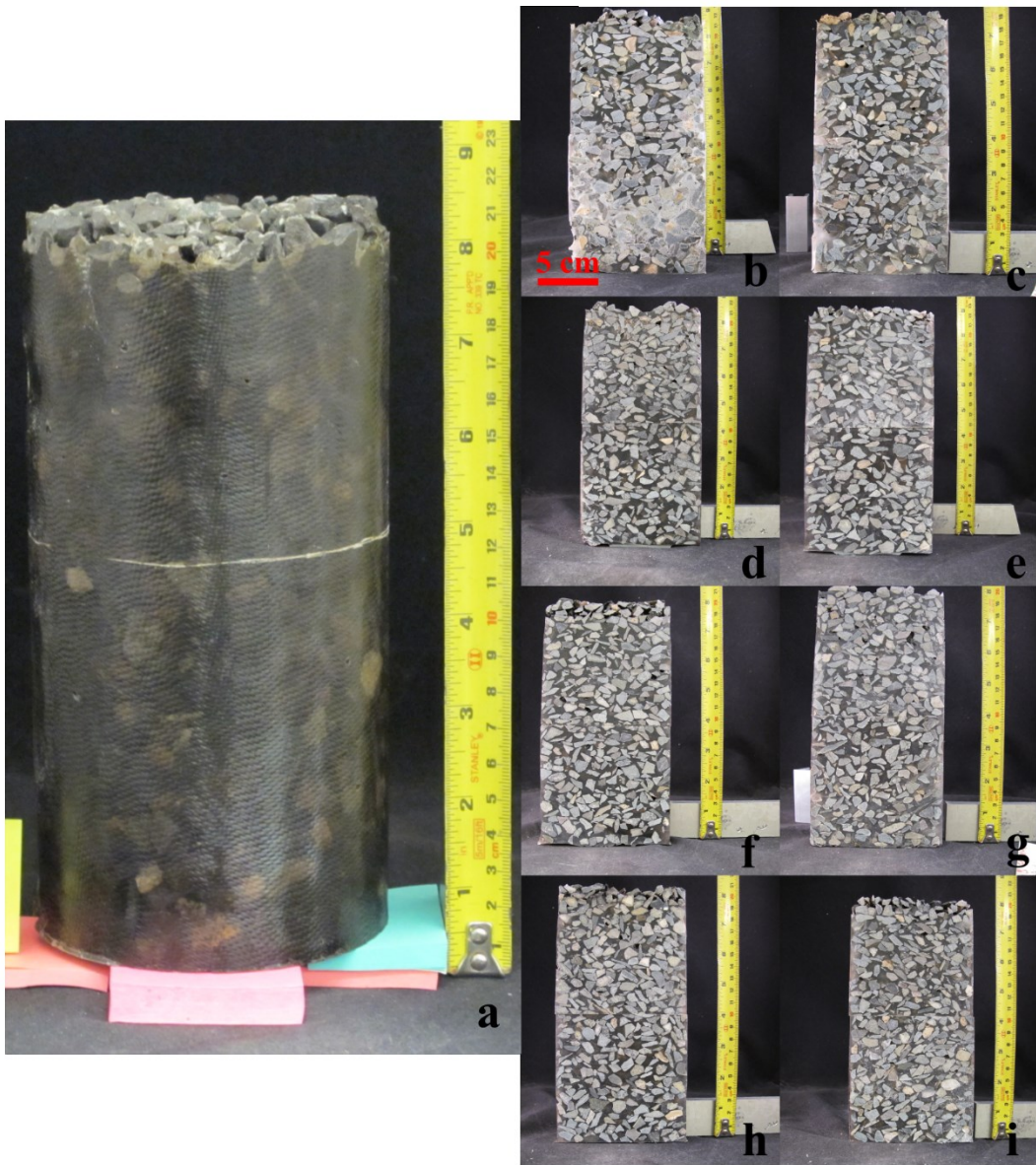


Figure 7: Photos of epoxied gravel pack samples showing: a) intact sample; b) cut water test; c) sawdust; d) fine + coarse microcellulose; e) cedar fiber; f) coarse microcellulose + cedar fiber 1; g) sawdust + cotton seed hulls; h) coarse microcellulose + cedar fiber 2; i) magma fiber.

To examine the LCM penetration into the gravel packs, the samples were dried for 24 hours at 60 °C then epoxied and allowed to dry at ambient conditions for ~72 hours to preserve the structure and LCM. Two epoxied samples were analyzed using a CT scan to find the internal porosity of each sample. The porosity of both was averaged to 45.5%, very close to the estimated porosity of 44.8% based on the gravel density and vessel internal volume. Once the epoxy set, the gravel packs were removed from the vessel and cut into sections.

Examples of the epoxied gravel pack and each cut sample are shown in Figure 7. Examining the internal structure of the gravel packs revealed a different story from the observations at the entrance to the gravel pack. With one exception, significant LCM penetration did not occur at all. The magma fiber traces were restricted to the top 0.5 cm of the gravel pack (Figure 7i), while the mixed materials in the sawdust + cotton seed hulls and coarse microcellulose + cedar fiber 2 samples only appeared penetrated ~1.5 cm into the samples (Figure 7g/h). The only exception to this is the fine microcellulose + coarse microcellulose test sample (Figure 7d). Coarse microcellulose is clear throughout the top of the sample, and can be seen as far as 6.5 cm from the top of the sample (Figure 8a). There are no obvious fine microcellulose particles trapped in the matrix.

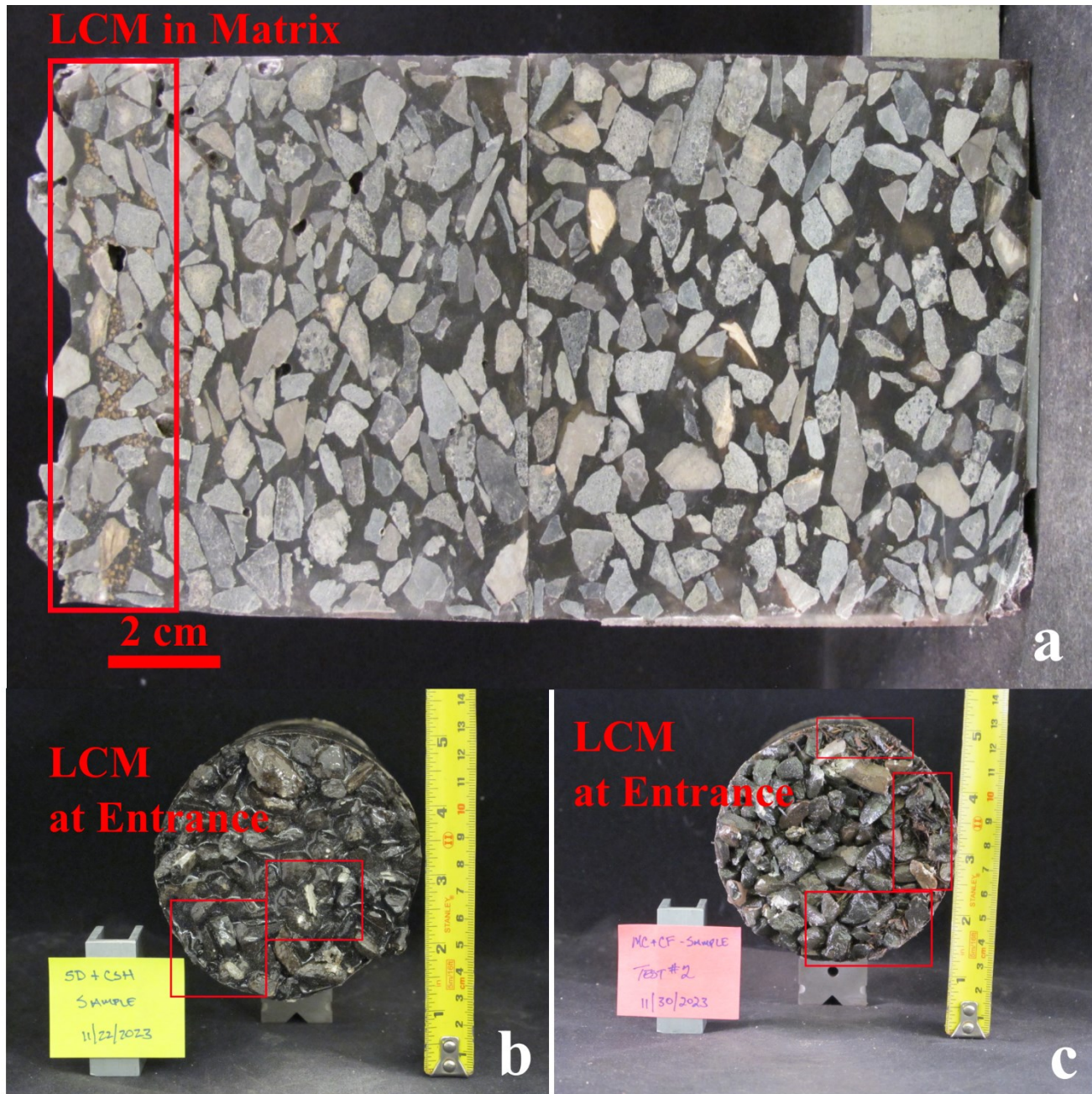


Figure 8: LCM trapped in epoxied samples: a) coarse microcellulose trapped in matrix; b) sawdust and cotton seed hulls at entrance to matrix; c) coarse microcellulose and cedar fiber at entrance to matrix.

4. DISCUSSION

Our results indicate a high variability in the clogging effectiveness of several types of LCM employed to cure LC encountered during geothermal drilling. Several types of LCM showed some degree of clogging behavior, but only when used as mixtures of multiple types of materials. Loepke et al. (1990) observed similar results to ours, noting that granular LCM and composites of flaky/fibrous and granular LCM were effective at clogging fractures up to a certain concentration. Through analysis of the post-test samples, it appears that most of the LCM act as bridges across the entrance to the gravel pack pore structure, and this is what primarily restricts flow. Evidence during testing suggests small particles (less than 400 μm) pass through the system without being stopped (e.g., small LCM fragments seen in catchment basin). The fact that the mixtures are more effective than the individual LCM suggests that to create blockage at the entrance to the loss zone, a long fibrous material is needed to create a bridge that is then filled or packed by smaller more flexible particles (Al-Defi and Al-Mahdawi, 2023), in absence of coarser particles such as drill cuttings (Nayberg and Petty, 1986).

The obvious exception to this is the rounded coarse microcellulose. While the fine microcellulose passed through the gravel pack due to its small grain diameter ($\sim 100 \mu\text{m}$), the coarse microcellulose was able to pass through the entrance pores but still clog at more restricted pathways. Unlike the other LCM, the granular geometry allowed the particles to pass more easily through the gravel pack but pile up at narrow restrictions in the system. Compared to single open fractures, in a geothermal reservoir, a highly fractured zone represented by a gravel pack has many such clogging points, thus the use of this type of LCM would lead to a wider zone of reduced permeability. Because such a zone would have reduced differential pressure gradient, the produced LCM “plug(zone)” would be more stable.

Despite the high-pressure buildup of the upstream fluid pressure, the coarse microcellulose particles from the experiment appear to be largely intact compared to untested grains. This may be attributed to the mechanical strength of the high-density particles, but may also be due to a better thermal degradation resistance. The sawdust and cotton seed hulls trapped in the gravel pack appear to be heavily altered by the temperature, showing a blackened structure that did not retain its original geometry, whereas the coarse microcellulose and cedar fiber appear to retain their shape, rigidity, and coloration (Figure 8). This is interesting because the fine microcellulose + coarse microcellulose and coarse microcellulose + cedar fiber 2 tests seemed to have the largest fluid pressure differences observed during testing (Table 2, Figure 5). Thermal degradation may play a role in reducing the clogging capability of softer LCM. The most significant example of this is the magma fiber test. Though initially this sample does not exhibit much flow restriction or pressure buildup, after a day of pumping clogging occurs. Magma fiber generally is considered a thermally stable material for use as an LCM, and is shown to have low degradation at high temperatures (Kibikas et al., 2023). However, moderate force or abrasion applied to magma fiber after heat exposure can disintegrate the material into a fine powder. The material observed on the gravel pack entrance coating the gravel is this residue, and the fibrous nature has been completely lost. These results suggest that the effect of temperature on LCM over time can have as much of an effect on the stability of an LCM bridge as the wellbore pressure. In order for an LCM to be effective for LC treatment in geothermal wells, they must be able to 1) create a bridge across a permeable zone; 2) withstand the pressure difference between the wellbore and the formation; 3) resist significant thermal degradation at geothermal conditions.

5. CONCLUSIONS

A high temperature flow loop system was developed to test clogging effectiveness at geothermal drilling conditions. Multiple LCM were tested in the system at high temperatures for up to 3 days. Pressure and flow data indicate the best results for testing come from mixtures of materials that 1) have moderate rigidity and 2) have a moderate resistance to thermal degradation. Analysis of the tested samples shows that clogging was most pervasive with granular microcellulose, which was able to create moderate but not total restriction of flow. Larger and softer LCM tended to bridge the entrance but likely break down under continued flow. For treating LC in geothermal wells, we suggest: 1) thermal degradation of LCM should be considered with respect to the downhole conditions; 2) large volumes of granular particles with smaller average diameters than the average fracture diameter be used; and 3) certain LCM may not be ideal due to their lower rigidity and inability to support pressure buildup.

ACKNOWLEDGEMENTS

The authors would like to thank Drs. John Tuttle and Ron Tate (Sinclair Well Products) for providing the commercial LCMs used in the research. The authors offer thanks to Jiann-cherng Su for conducting an internal review of this paper for Sandia National Laboratories. This work is supported by the U.S. Department of Energy, Office of Energy Efficiency and Renewable Energy (EERE), Office of Technology Development, Geothermal Technologies Office, under Award Number DE-AC02-05CH11231 with LBNL and contract DE-NA0003525 with SNL. Sandia National Laboratories is a multi-mission laboratory managed and operated by National Technology & Engineering Solutions of Sandia, LLC, a wholly owned subsidiary of Honeywell International Inc., for the U.S. Department of Energy’s National Nuclear Security Administration. This paper describes objective technical results and analysis. Any subjective views or opinions that might be expressed in the paper do not necessarily represent the views of the U.S. Department of Energy or the United States Government.

REFERENCES

Abrams, A.: Mud Design to Minimize Rock Impairment Due to Particle Invasion, *J. Petroleum Technology*, 29(5), (1977), 586-592.

Al-Delfi, A.K., and Al-Mahdawi, F.H.: A comprehensive review of lost circulation: Principles and treatments, *AIP Conference Proceedings*, 2839(1). AIP Publishing (2023).

Alsaba, M., Al Dushaishi, M.F., Nygaard, R., Nes, O.M., and Saasen, A.: Updated criterion to select particle size distribution of lost circulation materials for an effective fracture sealing, *Journal of Petroleum Science and Engineering*, 149, (2017), 641-648.

Blankenship, D.A., Wise, J.L., Bauer, S.J., Mansure, A.J., Normann, R.A., Raymond, D.W., and LaSala, R.J.: Research efforts to reduce the cost of well development for geothermal power generation. 40th ARMA US Rock Mechanics/Geomechanics Symposium, Anchorage, AK, ARMA/USRMS 05-884 (2005).

Cole, P., Young, K., Doke, C., Duncan, N., and Eustes, B.: Geothermal drilling: a baseline study of nonproductive time related to lost circulation, *Proceedings, 42nd Workshop on Geothermal Reservoir Engineering*, Stanford University, Stanford, CA (2017).

Kibikas, W., Chang, C., Bauer, S.J., Nakagawa, S., Kneafsey, T., Dobson, P., and Samuel, A.: Thermal degradation and mixture properties of materials used for lost circulation management, Proceedings, 48th Workshop on Geothermal Reservoir Engineering, Stanford University, Stanford, CA (2023).

Loepke, G., Glowka, D., and Wright, E.: Design and evaluation of lost-circulation materials for severe environments. *Journal of Petroleum Technology*, 42.03 328-337 (1990).

Lowry, T., Winn, C., Dobson, P., Samuel, A., Kneafsey, T., Bauer, S., and Ulrich, C.: Examining the Monetary and Time Costs of Lost Circulation, Proceedings, 47th Workshop on Geothermal Reservoir Engineering, Stanford University, Stanford, CA (2022).

Nakagawa, S., Chang, C., Kibikas, W., Kneafsey, T., Dobson, P., Samuel, A., and Bauer, S.J.: Laboratory evaluation of the short-term clogging behavior of various materials and their combined use for lost circulation management, Proceedings, 48th Workshop on Geothermal Reservoir Engineering, Stanford University, Stanford, CA (2023).

Nayberg, T. M., and Petty, B.R.: Laboratory study of lost circulation materials for use in oil-base drilling muds. In SPE Deep Drilling and Production Symposium, pp. SPE-14995. SPE (1986).

Price, C., Pyatina, T., Su, J.C., and Robey, R.E.: A Technology Roadmap for Advanced Geothermal Well Construction, Oak Ridge National Laboratory Report No. ORNL/TM-2023/2957 (2023).

Vickers, S., Cowie, M., Jones, T., and Twynam, A.J.: A New Methodology that Surpasses Current Bridging Theories to Efficiently Seal a Varied Pore Throat Distribution as Found in Natural Reservoir Formations, Paper AADE-06-DF-HO-16 presented at the AADE Fluids Conference, Houston, Texas, USA (2006).

Whitfill, D.: Lost Circulation Material Selection, Particle Size Distribution and Fracture Modeling with Fracture Simulation Software, Paper IADC/SPE 115039 presented at the IADC/SPE Asia Pacific Drilling Technology Conference and Exhibition, Jakarta, Indonesia (2008).

Winn, C., Dobson, P., Ulrich, C., Kneafsey, T., Lowry, T.S., Akerley, J., Delwiche, B., Samuel, A., and Bauer, S.: Context and mitigation of lost circulation during geothermal drilling in diverse geologic settings, *Geothermics*, 108, (2023), 102630.